DESIGN OF A HIGH-LIFT AIRFOIL FOR HANG-GLIDER APPLICATIONS

by Richard M. Howard

Department of Aeronautics and Astronautics, Naval Postgraduate School
Monterey, California

Abstract

The design requirements for an airfoil for hang-glider applications are reviewed. An airfoil design computer program was used to develop an airfoil providing a high maximum lift coefficient, a high lift-to-drag ratio, and a docile stall behavior, at a Reynolds number of 1 million. Comparisons to other low-Reynolds-number high-lift airfoils are made.

Nomenclature

c	—airfoil chord
C_L	—lift coefficient per unit span $= L/qc$
C_D	—drag coefficient per unit span $= D/qc$
D	—drag per unit span
L	—lift per unit span
q	— freestream dynamic pressure $= 1/2 \rho V_\infty^2$

Re   —Reynolds number $= V_\infty c / v$
V   — local velocity from potential flow calculations
V_∞ — freestream velocity
x   —streamwise coordinate
y   —transverse coordinate
α —angle of attack
v — coefficient of kinematic viscosity
p — air density

Introduction

Prior to the current decade, the choice of airfoils for general-aviation use was somewhat limited. Commercial aircraft companies developed their own airfoils for optimum transonic cruise, and there was little application of these airfoils for general low-speed use. An exception was the GA(W)-1 airfoil, now designated the LS(1)-0417. It was not uncommon for a small aircraft manufacturer or experimental homebuilder to select an airfoil with the text of Abbott and von Doenhoff[1] as the only available source. Of course, sailplane competition had long before driven soaring enthusiasts to consider more highly-optimized contours, resulting in the development of many excellent airfoils by Wortmann and Eppler. Recently, general and experimental aviation have made great gains in aerodynamic improvements with an increased interest in reduced viscous drag[2] and the design of a family of airfoils with natural laminar flow,[3] with research directed by NASA-Langley. Advances have also been made in the low-Reynolds-number flight regime, with the work of Selig[4] and with the publication of Eppler profiles.[5] Both of the latter relate to airfoils designed for model sailplanes, operating in the Reynolds-number regime of 60,000 to 500,000.

An area of airfoil development with less progress is that pertaining to foot-launched weight-shift-control flying wings, or hang gliders. The Reynolds numbers for hang gliders, due to their relatively large mean chords, range from 750,000 to 2 million. The recent general-aviation airfoils have been designed for a range of 3 to 9 million. Also, the requirements for hang gliders differ greatly from those for general aviation aircraft. A review of the design requirements relating to hang glider airfoils is given in the next sections.

General Design Requirements

A review of low-speed airfoil design is given by Miley.[6] In order for an airfoil to generate lift, there must exist at least one adverse pressure gradient on either the upper or lower surface. This requirement is demonstrated in the three airfoil types shown in Figure 1, taken from Reference 6.

Plotted is the velocity ratio (local to freestream) for the two surfaces versus dimensionless chord distance. Airfoil type 1 has a favorable pressure gradient over the entire lower surface at the design condition shown; lift is generated by the low pressure on the upper surface, which requires a strong adverse pressure gradient to recover to the freestream value. Airfoil type 2 uses strong pressure changes on both surfaces, but with more moderate adverse gradients. This type is the most common for aircraft application, due to its range of attached flow and its gentle stall behavior. Airfoil type 3 achieves lift from high pressure on the lower surface. At the same lift as the others, the recovery is the most moderate, and therefore this type can tolerate extremely low Reynolds numbers before laminar separation takes place. This type is identical to airfoil contours found on birds[7] — highly-cambered, thin sections. One problem with cambered lower surfaces, though, is the formation of laminar separation
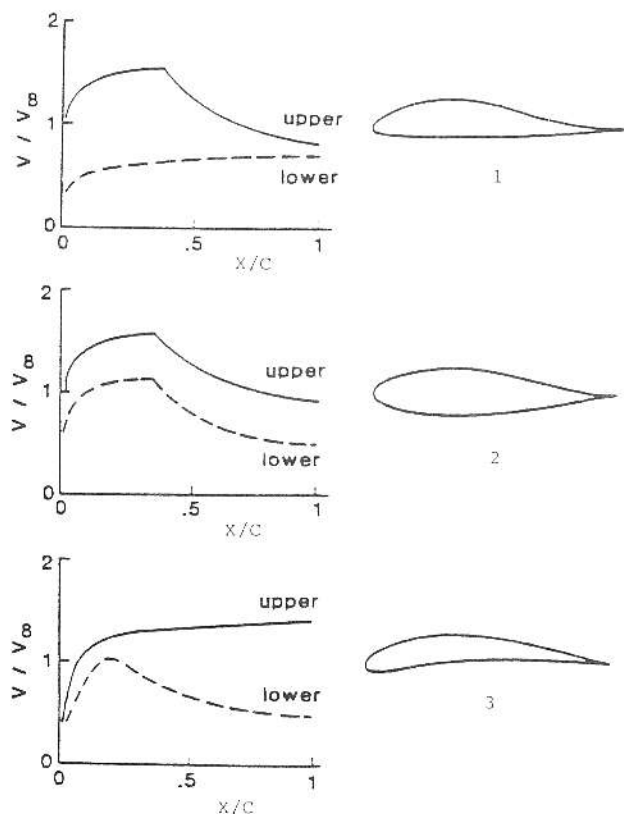

FIGURE 1. Three airfoil types and their velocity distributions. (Reference 6).

bubbles at low angles of attack, making for an inefficient high-speed condition.

Type 1 airfoils have been found to produce high lift efficiently at relatively low Reynolds numbers from 500,000 to 1 million. Air-foils of this type have been successfully designed by Liebeck,[8] Lis-saman,[9] and Miley,[10] and are generally referred to as "Liebeck [-type]" airfoils.

The general approach of type-1-airfoil design is: (1) to accelerate the flow quickly very near the leading edge on the upper surface; (2) to have a run of constant-pressure flow; (3) to have a short mild-adverse-pressure-gradient region over which the flow transitions to a turbulent state; and (4) to have a severe adverse-pressure-gradient region over which the flow returns to nearly freestream pressure. This extreme pressure-recovery method was first proposed by Stratford[11,12] as a way to return to freestream pressure over the shortest distance and with the minimum loss of energy. The application of this approach to airfoil design is discussed below.

Hang Glider Airfoil Design

The performance of hang gliders, most commonly measured in terms of lift-to-drag ratio, L/D, has drastically improved since early pioneers wrapped plastic sheeting around bamboo frames and leaped off of sand dunes. Current L/D's can be on the order of 10 to 12 for a hang glider of aspect ratio from 6 to 8. Rigid-wing hang gliders, with even higher aspect ratios, may reach values of 18.[13] Early single-surface hang gliders had upper surfaces similar to that for a Liebeck airfoil; but the lack of a lower surface (even with a double-surface leading edge) meant that the glider would be a poor performer at cross-country speeds. For the reason

mentioned for thin highly-cambered airfoils, drag would be high. The advent of 100 double-surfaced gliders meant that the airfoil technology for type-1 airfoils could be fully utilized.

Some rigid-wing gliders have used advanced airfoils, such as the Icarus V by Taras Kiceniuk in 1974, which used the TK 7315 airfoil developed by Liebeck and Lissaman.[13] Probably the most well-known of the low-speed high-lift airfoils is the L1003 by Liebeck,[14] which achieved a phenomenal maximum L/D of 220 at a Reynolds number of 1 million. The lift curve and drag polar for the Liebeck L1003 are shown in Figures 2 and 3. But the L1003 was designed for a laminar "rooftop"; that is, for a laminar constant-pressure region before the adverse pressure gradient. And though the airfoil was designed for a Reynolds number of 2 million, it was tested at a Reynolds number of 1 million, because freestream turbulence in the wind tunnel caused premature transition on the rooftop at higher Reynolds numbers. The suggestion is that with this early transition, airfoil performance was degraded. Sensitivity to freestream conditions (as well to contamination from bugs, etc.) must be considered in the adoption of an airfoil for current use.
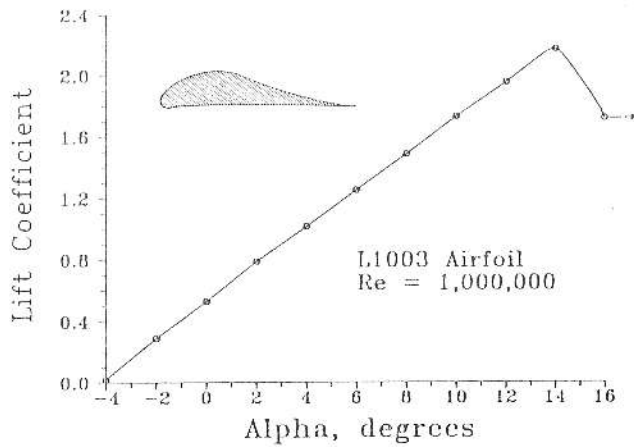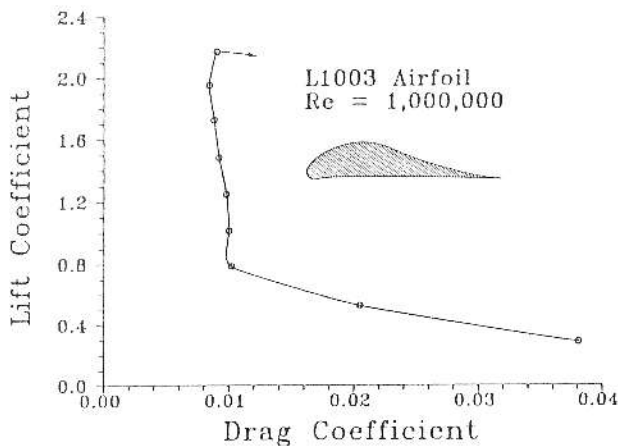
Another consideration in the use of a high-lift airfoil is its stall behavior. Liebeck, in the design of the L1003, applied a severe Stratford-type pressure distribution over the recovery region of the upper surface. This distribution is designed to maintain attached flow over that recovery region by a constant margin from separation. This means that when the aft section does separate, it should (by design) separate all at once. The test data for the L1003 airfoil indicate that this extreme behavior is at least partially realized, as the lift curve shows a very abrupt loss in lift at the stall. A gentler stall behavior is probably desired for an actual hang glider configuration. The purpose of Liebeck was to determine the maximum lift coefficient for a single-element airfoil at low Reynolds numbers, not to design a high-lift airfoil for practical application. More recent designs by Liebeck, such as the LNV109A,[15] are more practical air-foils. The LNV109A, at a Reynolds number of 650,000 and with a restricted pitching moment of -0.05, has a $C_{l_{max}}$ of 1.775 and a maximum L/D of 120.

HG(1)-1715 Airfoil

An airfoil design was requested by a hang glider manufacturer with the following characteristics. It should have very high L/D at high lift, but also at lower angles of attack. The stall behavior should be progressive. It was desired, for ease of manufacture (requiring straight ribs), that the recovery region of the upper section be as straight as possible (with little or no curvature). It was also noted that, because of the use of a mylar sheet leading edge and fabric pocket, a zig-zag stitch line exists slightly ahead of the point of minimum pressure on the upper surface (at about 16% chord), and at about 7% chord on the lower surface.

The resulting airfoil, designated the HG(1)-1715, is shown in Figure 4, and the velocity distribution at 8° angle of attack is shown in Figure 5. Coordinates for the airfoil are given in
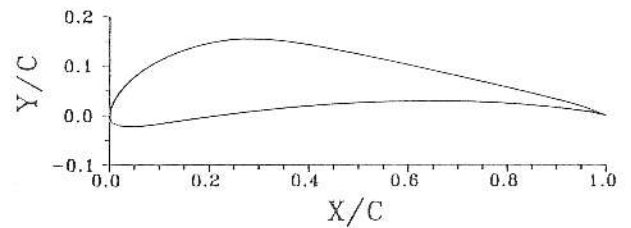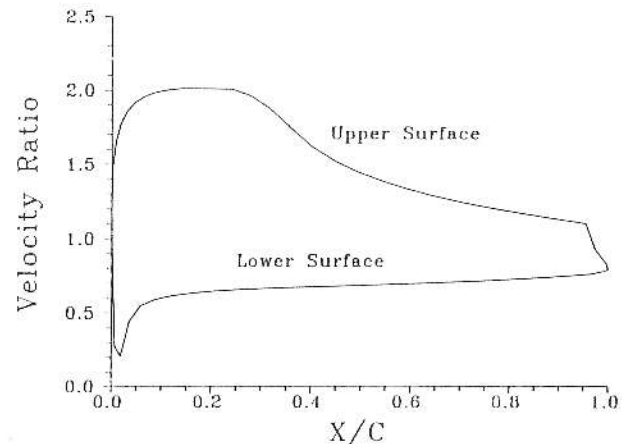

FIGURE 2. Lift curve for Liebeck L1003 airfoil. (Ref. 14).

FIGURE 4. HG(1)-1715 airfoil.

FIGURE 3. Drag polar for Liebeck L1003 airfoil (Ref. 14).

FIGURE 5. Velocity distribution at 8° angle of attack for HG(1)-1715 airfoil

TABLE 1. HG(1)-1715 airfoil coordinates

x	y	x	y
1.00000	0.00000	0.00792	0.02832
0.99662	0.00127	0.00222	0.01403
0.97308	0.01090	0.00002	0.00125
0.95434	0.01752	0.00141	-0.00913
0.93056	0.02453	0.00753	-0.01643
0.90170	0.03216	0.01921	-0.02090
0.86817	0.04051	0.03626	-0.02276
0.83041	0.04953	0.05898	-0.02182
0.78895	0.05919	0.08794	-0.01836
0.74436	0.06940	0.12327	-0.01328
0.69727	0.08006	0.16443	-0.00729
0.64834	0.09101	0.21081	-0.00086
0.59828	0.10208	0.26172	0.00560
0.54783	0.11306	0.31642	0.01176
0.49773	0.12369	0.37410	0.01731
0.44873	0.13364	0.43390	0.02198
0.40163	0.14252	0.49487	0.02553
0.35721	0.14966	0.55602	0.02783
0.31579	0.15403	0.61636	0.02885
0.27695	0.15496	0.67494	0.02861
0.24022	0.15242	0.73081	0.02722
0.20528	0.14681	0.78315	0.02484
0.17222	0.13876	0.83116	0.02169
0.14138	0.12869	0.87418	0.01800
0.11308	0.11692	0.91159	0.01402
0.08757	0.10376	0.94292	0.01002
0.06505	0.08949	0.96773	0.00626
0.04571	0.07446	0.98564	0.00304
0.02969	0.05900	0.99641	0.00081
0.01708	0.04348	1.00000	0.00000

Table 1. The airfoil was designed using the Eppler method which is documented in Reference 16. The method takes prescribed velocity-distribution characteristics to conformally-map the design-airfoil surface. The potential flow about the airfoil is solved by a panel method, and is combined with an integral-boundary-layer analysis to produce lift curve, drag polar, and transition and separation predictions. Based on the mean chord for a typical hang glider, the stall Reynolds number is about 1 million and the cruise Reynolds number 1.75 million. Results were run for these two cases; graphs are shown for the first case and some differences are noted for the latter.

From the airfoil contour, one can note that the upper surface is essentially straight from 40% to 90% chord, as desired in the design. The last few percent of chord is cambered for a consistent pressure recovery on both surfaces. It is expected that this camber would not be built into the actual configuration; in fact, it is expected that some reflex of the trailing edge would be necessary for proper trim conditions of the hang glider. Of course, the reflex would also serve to reduce the $C_{l,max}$ of the airfoil, as it effectively unloads the aft section.

The velocity distribution in Figure 5 is at a C_l near the design value of 1.7. The flow can be seen to accelerate to a velocity ratio of about twice the freestream value. After a run of constant pressure, the flow goes through a "transition ramp" and transitions to turbulent flow at about 26% chord. The flow then progresses through a concave pressure recovery with an abrupt recovery near the trailing edge. The lower surface is seen to slowly accelerate all the way to the trailing

edge. At this high C_l and angle of attack, the rise in velocity at the leading edge is still well-behaved and not "peaky."

Figure 6 shows the transition and separation characteristics for the two surfaces as functions of the arclength along each surface for a Reynolds number of 1 million. The angle of zero lift is -8.45°.
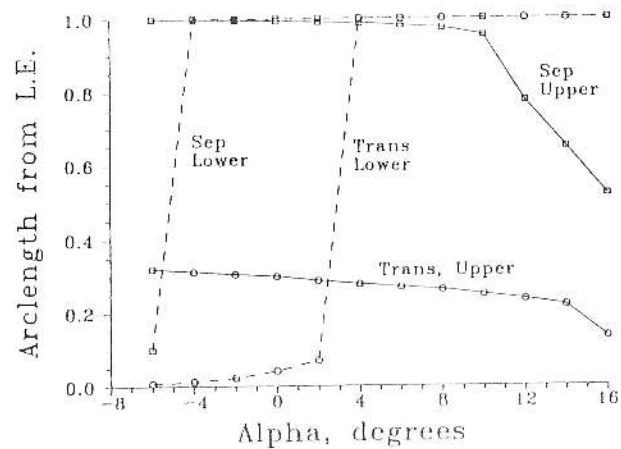

FIGURE 6. Predicted transition and separation characteristics for HG(1)-1715 airfoil.

First consider the upper surface. Transition from laminar to turbulent flow moves forward smoothly from 32% to 21% arclength as angle of attack increases from -6° to 14°. Separation on the upper surface stays within 5% of the trailing edge until an angle of attack of 10°, the condition of maximum lift, and 2.7° beyond the design point and the condition of maximum L/D. Looking at the lower surface, transition is seen to take place near the leading edge until 2° angle of attack is reached, at which point the flow over the lower surface becomes completely laminar. The flow remains laminar over the lower surface for all increasing angles of attack. The Eppler code predicts the existence of a separation bubble at -6° angle of attack on the lower surface, and turbulent separation at 10% chord. This lift coefficient would correspond to a high-speed condition at a speed 2.7 times the stall speed (based on the airfoil values), and provides the lower limit of the range over which the design is optimized. At any higher angles of attack, the flow remains attached until the trailing edge on the lower surface.
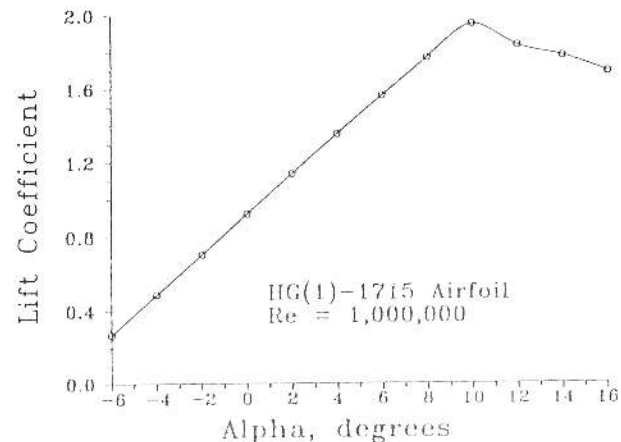

FIGURE 7. Lift curve for HG(1)-1715 airfoil.

The lift curve is shown in Figure 7. The maximum C_L predicted is 1.95 at Re=1 million and 2.08 at Re =1.75 million (not shown). To be noted is the gradual reduction in lift after the stall; no strong stall break is predicted. The actual design point where the maximum L/D is reached is at a C_L of 1.7, a safe margin below $C_{L_{max}}$. In the Eppler method described in Reference 16, the boundary-layer characteristics are calculated from the potential-flow pressure distribution; no iteration between the boundary-layer displacement thickness and the pressure distribution is performed. Boundary-layer codes cannot solve through a separated region; here, viscous corrections are applied to take the boundary-layer separation into account. Correlation between analytical and experimental results through stall using this method have been good; see Reference 17 for an example.

Figure 8 shows the drag polar for the airfoil. The dotted line at the low end of the lift range is to indicate that separation is predicted, with a higher drag expected than can be accurately determined in the code. The drag is fairly constant over the range from a C_L of 0.5 to 1.35. The reduction in value at C_L = 1.35 is due to the lower surface becoming completely laminar at this angle of attack. Between a C_L of 1.3 and the maximum value of 1.95, the slope of the polar is almost identical with the slope of a line drawn from the true origin to the polar, indicating a nearly-constant value of $(L/D)_{max}$ over this C_L range. The design condition falls nearly in the middle of this range, providing a constant value of $(L/D)_{max}$ even at an off-design C_L. This broad range for the maintenance of $(L/D)_{max}$ can be seen in the plot of L/D in Figure 9. The value at the design C_L is 124, and the curve is so broad such that the value of L/D remains above 120 for a C_L between 1.5 and 1.9.

The HG(1)-1715 is obviously optimized for high lift—with a CL_{max} of 1.95 and an L/D of 124 at CL = 1.7 at the design Reynolds number of 1 million. At half the lift coefficient, the value of L/D is still 77. Of course, these are two-dimensional values, and the airfoil must be integrated into a hang glider design for the configu-ration lift-to-drag ratios. The airfoil designation follows current NASA practice: "HG" for hang glider, "(1)" for the first in the series, "17" for the design C_L of 1.7 (where L/D is a maximum), and "15" for 14.8% maximum thickness.

Tripped Boundary Layer Results

What happens if both the upper- and lower-surface boundary layers are tripped to become turbulent at the locations of
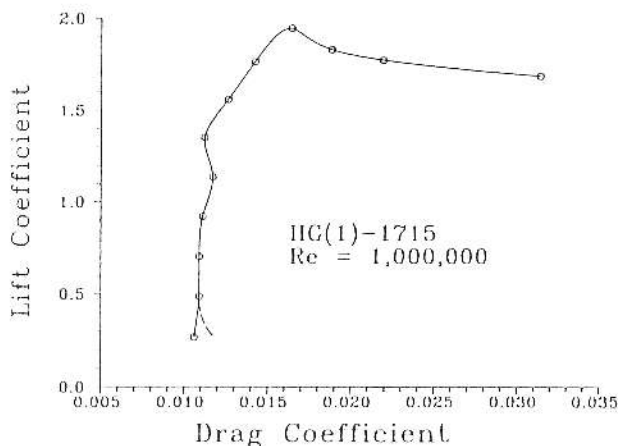

FIGURE 8. Drag polar for HG(1)-1715 airfoil.

the stitching? If fixed transition is assumed, at 6° angle of attack the drag over the upper surface increases by 40%, while over the lower surface it increases by a factor of 2.4 (though initially still at a low value), with a resulting 50% increase in airfoil C_D. It is not known whether the stitches would in fact trip the boundary layer. For a roughness less than a critical Reynolds number based on the roughness height, no effect will be made on the location of natural transition. The value for the critical Reynolds number based on the local flow conditions at the top of the roughness is approximately 600.[18] Work has also been done looking at the effects of insect debris contamination on transition location.[2] It was found that only 25% of the insects collected during the experiment actually tripped the boundary layer. For insect excrescence below a certain height, the boundary layer remains laminar. If it turns out that the stitches might be tripping the boundary layer, it would be helpful to locate the upper stitch at or near the naturally-occurring transition point, and either move the lower stitch to the stagnation point, or get rid of it altogether.
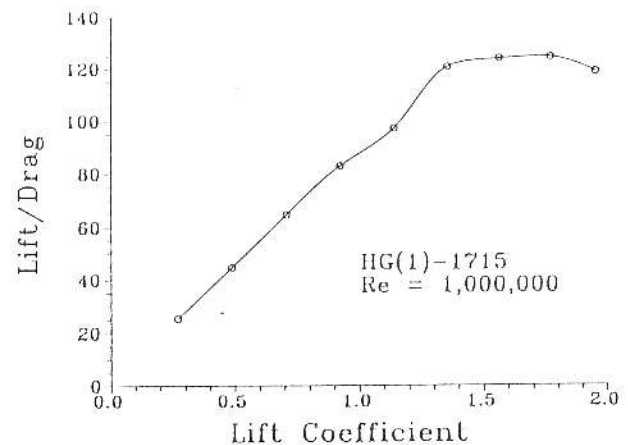

FIGURE 9. Lift-to-drag ratios for HG(1)-1715 airfoil.

Summary

Development of high-lift airfoils for hang-glider applications has not kept pace with that for competition sailplanes. An airfoil, designated the HG(1)-1715, has been designed at a Reynolds number of 1 million with a maximum C_L of 1.95, a value of L/D of 124 at a C_L of 1.7, a value of L/D of 120 over the range of C_L from 1.5 to 1.9, and a stall behavior gentler than for an airfoil with a severe Stratford pressure distribution. It is expected that continued competition in the sport of light foot-launched gliders will spur the development of more airfoil designs and other aerodynamic improvements as well.

References

[1]Abbott, Ira H., and von Doenhoff, Albert E., Theory of Wing Sections, McGraw-Hill, New York, 1949.

[2]Holmes, Bruce J., Obara, Clifford J., Gregorek, Gerald M., Hoffman, Michael J., and Freuhler, Rick J., "Flight Investigation of Natural Laminar Flow on the Bellanca Skyrocket II," SAE Paper 830717, April 1983.

[3]Somers, Dan M., "Design and Experimental Results for a Flapped Natu-ral-Laminar-Flow Airfoil for General Aviation Applications, NASA TP 1865, June 1981.

[4]Selig, Michael S., The Design of Airfoils at Low Reynolds Numbers," AIAA Paper 85-0074, January 1985.

[5]Thies, Werner, Eppler-Profile, Verlag Fur Technik und Handwerk, Germany, 1986.

[6]Miley, S.J., A Catalog of Low Reynolds Number Airfoil Data for Wind Turbine Aplications, Department of Aerospace Engineering, Texas A&M University, College Station, Texas, February 1982, pp. 19-23.

[7]Tucker, Vance A., and Parrott, G. Christian, "Aerodynamics of Gliding Flight in a Falcon and Other Birds," Journal of Experimental Biology, Vol. 52, No. 2, April 1970, pp. 345-367.

[8]Liebeck, Robert H., "A Class of Airfoils Designed for High Lift in Incompressible Flow," Journal of Aircraft, Vol. 10, No. 10, October 1973, pp. 610-617.

[9]Lissaman, P.B.S., "Low-Reynolds-Number Airfoils," Annual Review of Fluid Mechanics, Vol. 15, 1983, pp. 223-239.

[10]Miley, Stanley Jay, "An Analysis of the Design of Airfoil Sections for Low Reynolds Numbers, " Ph.D. Dissertation, Mississippi State University, State College, Mississippi, January 1972.

[11]Stratford, B.S., "The Prediction of Separation of the Turbulent Boundary Layer," Journal of Fluid Mechanics, Vol. 5, Pt. 1, January 1959, pp. 1-16.

[12]Stratford, B.S., "An Experimental Flow with Zero Skin Friction Throughout Its Region of Pressure Rise," Journal of Fluid Mechanics, Vol. 5, Pt. 1, January 1959, pp. 17-35.

[13]Rhodes, Chuck, "The Nimbus Sailplane," Whole Air Magazine, date not known, pp. 38-39.

[14]Liebeck, Robert H., "On the Design of Subsonic Airfoils for High Lift," Douglas Paper 6463, Douglas Aircraft Company, presented at the AIAA 9th Fluid and Plasma Dynamics Conference, San Diego, CA, July 1976.

[15]Liebeck, R.H., and Camancho, P.P., "Airfoil Design At Low Reynolds Number with Constrained Pitching Moment," Proceedings of the Conference on Low Reynolds Number Airfoil Aerodynamics, UNDAS-CP-77B123, University of Notre Dame, Notre Dame, IN, June 1985, pp. 27-51.

[16]Eppler, Richard, and Somers, Dan M., A Computer Program for the Design and Analysis of Low-Speed Airfoils," NASA TM 80210, 1980.

[17]Somers, Dan M., "Design and Experimental Results for a Natural-Laminar-Flow Airfoil for General Aviation Applications," NASA TP 1861, June 1981, pp. 88.

[18]Braslow, Albert L., Hicks, Raymond M., and Harris, Roy V. Jr., "Use of Grit-Type Boundary-Layer-Transition Trips on Wind-Tunnel Models," NASA TN D-3579, September 1966.